ACADÉMIE
DES SCIENCES
INSTITUT DE FRANCE

Comptes Rendus
Mécanique

Badr Kaoui

Multiphysics simulations in biomedical: fluid–structure interaction coupled with mass transfer

Volume 353 (2025), p. 779-790

Online since: 25 June 2025

https://doi.org/10.5802/crmeca.304

The Comptes Rendus. Mécanique *are a member of the Mersenne Center for open scientific publishing*
www.centre-mersenne.org — e-ISSN : 1873-7234

ACADÉMIE DES SCIENCES
INSTITUT DE FRANCE

Comptes Rendus. Mécanique
2025, Vol. 353, p. 779-790
https://doi.org/10.5802/crmeca.304

Review article / *Article de synthèse*

Multiphysics simulations in biomedical: fluid–structure interaction coupled with mass transfer

Simulations multiphysiques en biomédical : interaction fluide-structure couplée au transfert de masse

Badr Kaoui [a]

[a] Equipe Interactions Fluides Structures Biologiques (IFSB), Laboratoire Biomécanique et Bioingénierie (BMBI), UMR 7338 - Centre National de la Recherche Scientifique (CNRS) & Université de Technologie de Compiègne (UTC), 60200 Compiègne, France

E-mail: badr.kaoui@utc.fr

Abstract. We propose numerical schemes to study complex multiphysics problems involving fluid–structure interaction (FSI) coupled with mass/heat transfer (HMT). We primarily use the Lattice Boltzmann Method (LBM) to compute fluid flow and the advection–diffusion–reaction of chemical entities. The dynamics and deformation of structures are computed using the Lattice Spring Method (LSM), and we implement the Immersed Boundary Method (IBM) to achieve two-way coupling of fluid–structure interaction. For biomedical applications, we study controlled drug delivery from particles subjected to flow, passage of soft particles through microfluidic constrictions, performance of artificial pancreas-on-chip, as well as contraction–relaxation of lymphatic vessels and the opening–closing of their valves.

Résumé. On propose des schémas numériques pour étudier des problèmes multiphysiques complexes impliquant l'interaction fluide-structure (IFS) couplée au transfert de masse et de chaleur (TMC). On utilise principalement la méthode de Boltzmann sur réseau (LBM) pour simuler l'écoulement des fluides ainsi que l'advection-diffusion-réaction d'entités chimiques. La dynamique et la déformation des structures sont calculées à l'aide de la méthode des ressorts sur réseau (LSM), et on met en œuvre la méthode de la frontière immergée (IBM) pour assurer le couplage bidirectionnel de l'interaction fluide-structure. Dans le cadre des applications biomédicales, on étudie la libération contrôlée de médicaments à partir de particules soumises à un écoulement, le passage de particules déformables à travers des constrictions microfluidiques, la performance de pancréas artificiels sur puce, ainsi que la contraction-relaxation des vaisseaux lymphatiques et l'ouverture-fermeture de leurs valves.

Keywords. CFD, FSI, Multiphysics simulations, HPC, Biofluids, Biomedical engineering.

Mots-clés. Mécanique des fluides numérique, IFS, Simulations multiphysiques, Calcul haute performance, Biofluides, Génie biomédicale.

Funding. National Research Agency for funding the MechLymph (ANR-20-CE45-0008-01), UC-DC (ANR-23-CE51-0057), SOCA (ANR-24-CE06-6245-02), GENCI-IDRIS (Grant 2024-[AD012A13687R2]).

Manuscript received 24 February 2025, revised 20 May 2025, accepted 21 May 2025.

1. Introduction

In our modern world, scientists and engineers are increasingly faced with solving complex problems that involve multiple phenomena occurring at multiple scales and simultaneously. In biomedical engineering, the use of modeling and computer simulations has gained growing trust among researchers. These simulations are increasingly employed to assist in experiment planning and to elucidate the relationships and interactions between different elements and factors in biological, biomedical and biomimetic systems. While powerful commercial software solutions are available on the market, they are primarily designed to meet the needs of the aerospace and automotive industries. This highlights the necessity of developing in-house numerical codes tailored to the specific requirements of biomedical engineering research, and enabling high-performance multiphysics simulations. The following sections present the numerical techniques we use for biomedical applications, which can also be adapted and applied to other scientific domains and industrial sectors. Most biological and biomedical systems involve transport phenomena, including fluid flow, biochemical species transport, and interactions with deformable structures (see Figure 1). Additionally, these systems operate under the influence of external stimuli, such as applied flow or variations in ambient temperature.

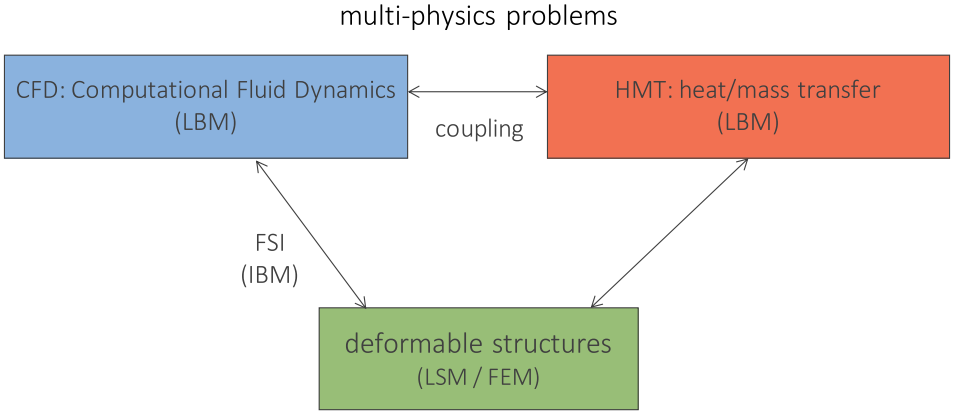

Figure 1. Coupling of the numerical methods used for solving each part and module of a multiphysics problem.

2. Transport phenomena

The flow of an incompressible Newtonian Fluid is governed by the Navier–Stokes equations,

$$\frac{\partial \mathbf{u}}{\partial t} + \mathbf{u}\cdot\nabla\mathbf{u} = -\frac{1}{\rho}\nabla p + \nu\nabla^2\mathbf{u} + \mathbf{f}, \tag{1}$$

$$\nabla\cdot\mathbf{u} = 0, \tag{2}$$

and the transport of chemical entities by the advection–diffusion–reaction equation,

$$\frac{\partial c}{\partial t} + \mathbf{u}\cdot\nabla c = \nabla\cdot(D\nabla c) + S, \tag{3}$$

where ρ and ν are respectively the density and the kinematic viscosity of the studied fluid (the solvent). D is the diffusion coefficient of the solute. The unkown solutions of these equations are the velocity field $\mathbf{u}(\mathbf{x}, t)$, the pressure field $p(\mathbf{x}, t)$ and the concentration field $c(\mathbf{x}, t)$, where $\mathbf{x}$ is the position and t the time. $\mathbf{f}$ represents a body force acting on the fluid, and S is a source term.

Instead of solving these partial differential equations directly, for example, using the Finite Element Method (FEM), we use an alternative approach: the Lattice Boltzmann Method (LBM) to compute the solutions [1–3]. This method is well suited for predicting the dynamics of complex fluids (e.g., particle suspensions, multiphase fluids) and computing flows in complex geometries (e.g., porous media, microfluidic systems).

Initially developed by physicists to overcome the drawbacks of the Lattice Cellular Automata method [2], such as the lack of Galilean invariance, the Lattice Boltzmann Method is now widely used by scientists and engineers. Here, we will not present the theoretical foundations of the method, but rather explain its principles and how it works.

The distinctive feature of LBM lies in the use of a distribution function that represents the probability of finding a fluid packet (pseudo-particles) at a position $\mathbf{x}$, at time t and with a discrete velocity direction $\mathbf{e}_i$. In LBM, both position and velocity (momentum) spaces are discretized, with $\Delta x = \Delta y = \Delta z = 1$ and $\Delta t = 1$. The evolution over time of the distribution f_i is given by the so-called Lattice Boltzmann equation,

$$f_i(\mathbf{x}+\mathbf{e}_i, t+1) - f_i(\mathbf{x}, t) = \Omega_i(\mathbf{x}, t), \tag{4}$$

with the left-hand side describing the streaming step of f_i, and the right-hand side representing the collision step through the operator Ω_i. Two types of operators are widely used: BGK and MRT. The BGK (Bhatnagar–Gross–Krook) operator is given by,

$$\Omega_i(\mathbf{x}, t) = -\frac{f_i - f_i^{\mathrm{eq}}}{\tau_f}, \tag{5}$$

where τ_f is the relaxation time required for f_i to tend toward its equilibrium function,

$$f_i^{\mathrm{eq}}(\mathbf{x}, t) = \omega_i \rho [1 + 3(\mathbf{u}\cdot\mathbf{e}_i) + \tfrac{9}{2}(\mathbf{u}\cdot\mathbf{e}_i)^2 - \tfrac{3}{2}(\mathbf{u})^2], \tag{6}$$

where ω_i are the weights associated to the type of the used lattice, see Figure 2. The microscopic physical quantity τ_f is related to the macroscopic physical quantity, the kinematic viscosity of the fluid ν, through the formula,

$$\nu = \tfrac{1}{3}(\tau_f - \tfrac{1}{2}). \tag{7}$$

Thus, τ_f can only take values greater than $1/2$, and when τ_f approaches $1/2$, numerical instabilities arise. The remedy for this issue is the use of the Multiple-Relaxation-Time (MRT) operator, which introduces different relaxation times for each velocity direction $\mathbf{e}_i$.

The non-slip boundary condition on the solid walls of the domain, $\mathbf{u} = 0$, is set using the bounce-back step in the LBM: the distribution function is reflected in the opposite direction ($\mathbf{e}_{-i}$) to the incident velocity direction ($\mathbf{e}_i$) if the position $\mathbf{x}$ is a solid node,

$$f_{-i}(\mathbf{x}+\mathbf{e}_{-i}, t+1) = f_i(\mathbf{x}, t). \tag{8}$$

There are also boundary conditions to be set at the inlet and the outlet of the domain. These can be periodic or of the Zou and He type [4], which allow for setting either velocities or pressures at the boundaries of the computational domain.

The local pressure and velocity of the fluid are evaluated respectively by the equation of state of the fluid and the first moment of the distribution f_i,

$$p(\mathbf{x}, t) = \frac{1}{3}\sum_i f_i(\mathbf{x}, t) = \frac{1}{3}\rho(\mathbf{x}, t), \tag{9}$$

$$\mathbf{u}(\mathbf{x}, t) = \frac{1}{\rho(\mathbf{x}, t)}\sum_i f_i(\mathbf{x}, t)\mathbf{e}_i. \tag{10}$$

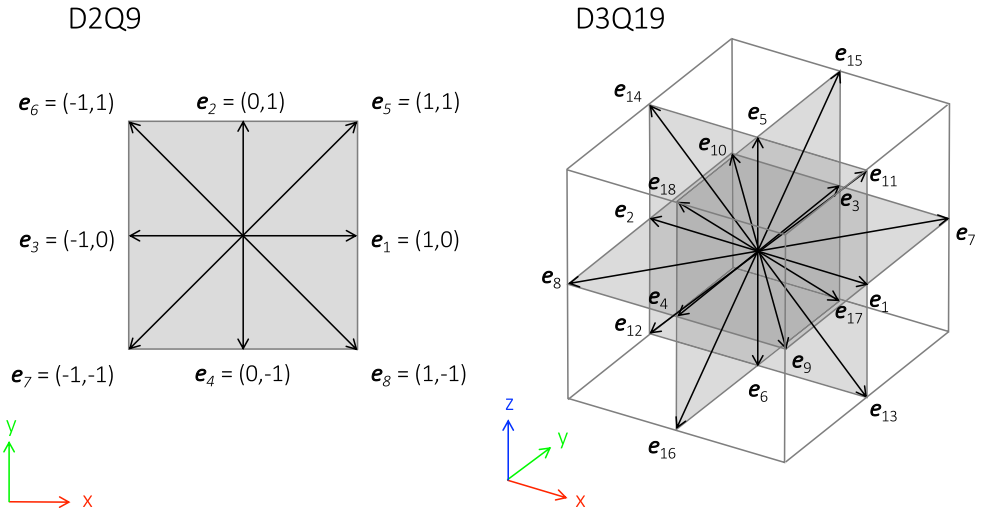

Figure 2. D2Q9 lattice (two-dimensional space, 2D, with 9 velocity directions, Q9) and D3Q19 lattice (three-dimensional space, 3D, with 19 velocity directions, Q19).

The LBM is also used to compute numerically the solution of the advection–diffusion–reaction equation [5–7]. To achieve this, an additional Lattice Boltzmann equation is introduced to govern the dynamics of another distribution function, g_i, associated with mass transfer,

$$g_i(\mathbf{x}+\mathbf{e}_i, t+1) - g_i(\mathbf{x}, t) = -\frac{g_i - g_i^{\mathrm{eq}}}{\tau_g}, \tag{11}$$

whose relaxation time τ_g is related to the solute diffusion coefficient D through the formula,

$$D = \tfrac{1}{3}(\tau_g - \tfrac{1}{2}), \tag{12}$$

and the concentration is given by the zero-th moment of g_i,

$$c(\mathbf{x}, t) = \frac{1}{3}\sum_i g_i(\mathbf{x}, t). \tag{13}$$

In 2D, the D2Q9 lattice is used with 9 velocity directions ($i = 0$–8), and in 3D, the D3Q19 lattice is considered with 19 velocity directions ($i = 0$–18), see Figure 2. The weights of these two lattices are,

$$\text{2D:}\quad \omega_i = \begin{cases} 4/9, & \text{for } i = 0, \\ 1/9, & \text{for } i = 1\text{–}4, \\ 1/36, & \text{for } i = 5\text{–}8. \end{cases} \tag{14}$$

$$\text{3D:}\quad \omega_i = \begin{cases} 1/3, & \text{for } i = 0, \\ 1/18, & \text{for } i = 1\text{–}6, \\ 1/36, & \text{for } i = 7\text{–}18. \end{cases} \tag{15}$$

The numerical stability of the LBM solver for the mass transfer part is further enhanced by using the same lattice as that of the LBM flow solver [5]. Moreover, this strategy enables the development of modular and ergonomic computer codes.

The body force $\mathbf{f}$ in the Navier–Stokes equations, the source term S in the advection–diffusion–reaction equation, and the boundary conditions vary depending on the studied problem. In LBM, $\mathbf{f}$ is accounted for by adding the term $3\omega_i(\mathbf{f}\cdot\mathbf{e}_i)$ to the right-hand side of Equation (8) [8], while S is incorporated by adding the term $\omega_i S$ to the right-hand side of Equation (11) [7].

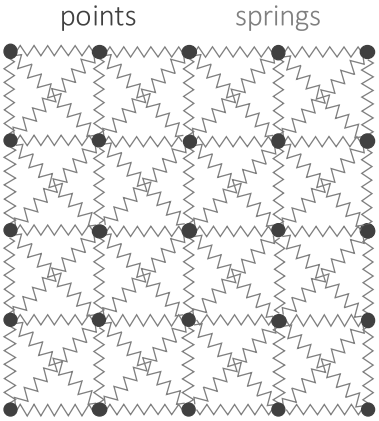

Figure 3. Two-dimensional network of points interconnected by Hookean springs of rigidity κ.

3. Deformable structures

The mechanics of deformable structures are governed by different elasticity laws. We are particularly interested in structures whose thickness is negligible compared to their size. We model them as two-dimensional structures of zero thickness. These structures evolve in three-dimensional space and are subjected to three deformation modes under the action of applied stresses: compression–dilation, shear and bending. For each mode, the structure exerts in turn a restoring force to recover its equilibrium shape at rest.

For small deformation regimes (e.g., Ref. [9]), we use the Lattice Spring Method (LSM) [10], which models the structure as a network of points interconnected by springs, see Figure 3. The mechanics of this network, at the microscopic scale, is capable of reproducing faithfully the mechanical behavior of the structure at the macroscopic scale. Each point i in the network experiences a force from its neighboring points j, governed by Hooke's law,

$$\mathbf{F}(i) = -\kappa \sum_{j \neq i} [d(i,j) - d_0(i,j)] \frac{\mathbf{r}(i,j)}{\|\mathbf{r}(i,j)\|}, \tag{16}$$

where κ is the spring rigidity, d and d_0 are the current and initial distances between points i and j, respectively, and $\mathbf{r}$ the position vector connecting these points. Other types of spring networks can be used, such as the one generated by triangular meshing of the domain. The constant κ can be related and estimated from the macroscopic elastic moduli of a material, such as Young's modulus, depending on the lattice type [11].

For problems involving large deformation regimes (e.g., Refs. [12–14]), models derived from continuum mechanics are more suitable, as they allow for the consideration of the nonlinear elasticity of structures. For instance, the Neo-Hookean law, which describes the energetic cost of the shear deformation mode,

$$E_{\mathrm{s}} = \frac{\kappa_{\mathrm{s}}}{2} \int_A \left[I_1 - 1 + \frac{1}{I_2 + 1} \right] \mathrm{d}A, \tag{17}$$

where κ_{s} is the shear modulus, $I_1 = \lambda_1^2 + \lambda_2^2 - 2$ and $I_2 = \lambda_1^2 \lambda_2^2 - 1$ are the two strain invariants, λ_1 and λ_2 are the principal stretch ratios. A and $\mathrm{d}A$ are the surface area and surface element of the structure, respectively. We evaluate this energy using FEM.

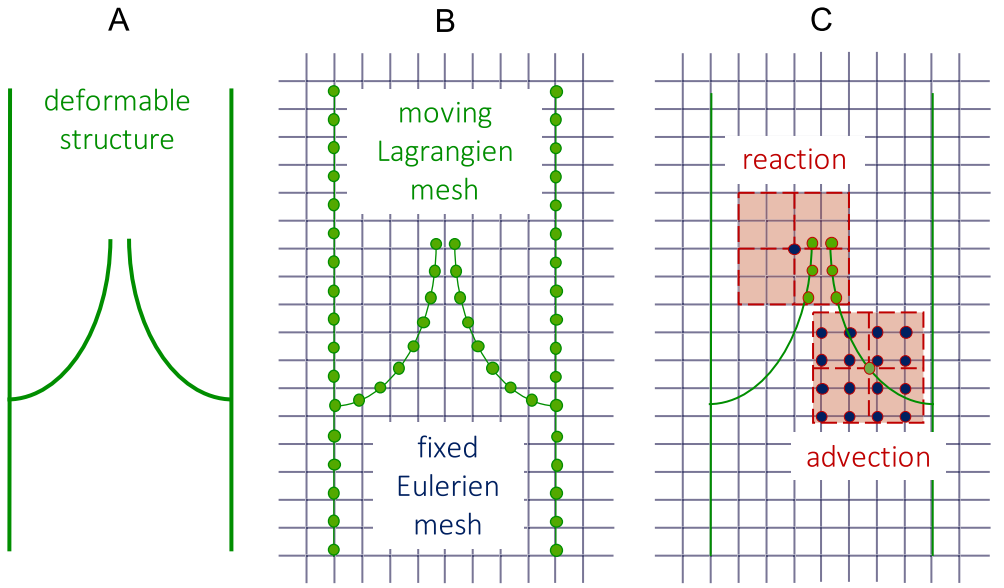

Figure 4. (A) Deformable structure, here a vessel with a bi-leaflet valve. (B) Discretization of the structure into points interconnected by springs (moving Lagrangian mesh), immersed in a fixed grid on which the flow is computed (fixed Eulerian mesh). (C) Nodes used by the Immersed Boundary Method for interpolating velocities onto the structure and extrapolating forces to the fluid nodes.

4. Fluid–structure interaction

Coupling between structure dynamics and fluid flow, known as fluid–structure interaction (FSI), is achieved using the Immersed Boundary Method (IBM) [15–17]. In this method, the structure is represented by a mobile Lagrangian mesh, immersed in a stationary Cartesian Eulerian mesh, where the flow is computed. See the illustration in Figure 4 for the 2D case.

Physical quantities calculated at a point $\mathbf{r}_1 \equiv (x_1, y_1, z_1)$ of one mesh are communicated to a point $\mathbf{r}_2 \equiv (x_2, y_2, z_2)$ of the other mesh by interpolation or extrapolation using a Dirac-type function Δ, see Figure 5. In 3D, we use,

$$\Delta(\mathbf{r}_1, \mathbf{r}_2) = \delta(x_1, x_2)\delta(y_1, y_2)\delta(z_1, z_2), \tag{18}$$

with,

$$\delta(a, b) = \begin{cases} \dfrac{1}{4}\left(1 + \cos\dfrac{\pi(a-b)}{2}\right) & \text{if } |a-b| \le 2, \\ 0 & \text{otherwise.} \end{cases} \tag{19}$$

The velocity $\mathbf{v}$ of a point $\mathbf{r}$ on the structure is thus evaluated by interpolating the velocities $\mathbf{u}$ computed at the surrounding fluid points $\mathbf{x}$ (see Figure 4C—advection),

$$\mathbf{v}(\mathbf{r}, t) = \sum_{\mathbf{x}} \Delta(\mathbf{r}, \mathbf{x})\mathbf{u}(\mathbf{x}, t). \tag{20}$$

This is the velocity used to move each point of the Lagrangian mesh, for example, using the Euler scheme, under the assumption that inertial effects are negligible,

$$\mathbf{r}(t+1) = \mathbf{r}(t) + \mathbf{v}(\mathbf{r}, t). \tag{21}$$

The displacements of all the points cause the structure to evolve as a whole towards an out-of-equilibrium shape. As a result, the structure exerts a reaction force on the fluid, thereby

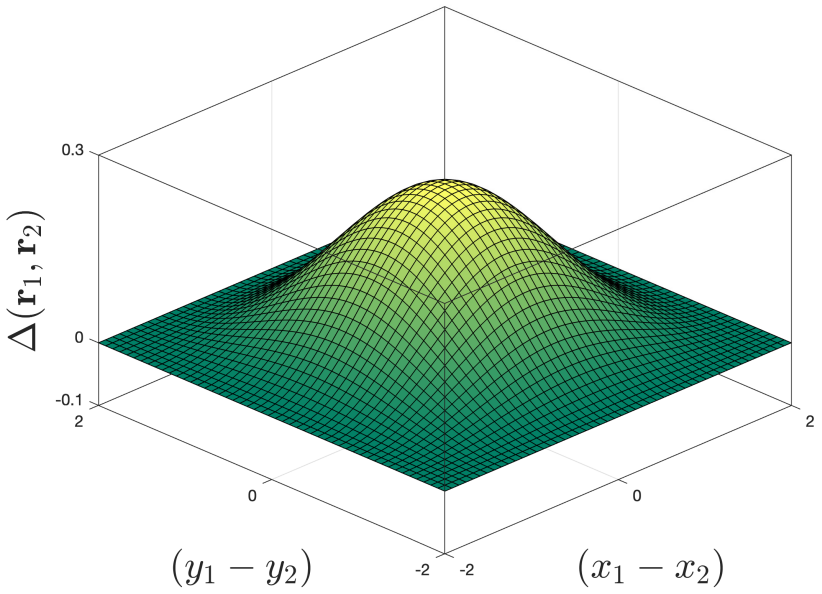

Figure 5. The Δ function used by IBM in 2D.

perturbing and altering the flow in its vicinity. The force **F** exerted by a point **r** of the structure is distributed by extrapolation to the nearby fluid points **x** (see Figure 4C—reaction),

$$\mathbf{f}(\mathbf{x}, t) = \sum_{\mathbf{r}} \Delta(\mathbf{r}, \mathbf{x}) \mathbf{F}(\mathbf{r}, t). \tag{22}$$

5. Multiphysics coupling

The three numerical methods, LBM, LSM (or FEM) and IBM, are coupled and executed following an explicit time-stepping scheme. Each iteration in the main code is structured into three distinct blocks: the LBM block for the transport phenomena part (CFD and/or HMT), the LSM block for the structure mechanics part (Structure), and the IBM block for the two-way FSI coupling, organized into two levels: advection and reaction.

The LBM and LSM blocks operate independently without direct interaction. It is the IBM block that ensures the coupling between the LBM and LSM. This two-way coupling enables the flow to advect and deform the structure (fluid–structure interaction), while also accounting for the flow disturbance caused by the presence of the structure (structure–fluid interaction). The various execution steps of a typical computer code of multiphysics coupling are outlined in the flowchart in Figure 6. The main challenge in this multiphysics coupling explicit scheme lies in identifying suitable numerical values for the key parameter set, particularly the coupling coefficients, to ensure numerically stable simulations. This involves trial-and-error tuning of physical and numerical parameters, estimation of key dimensionless numbers relevant to the problem, and analysis of the relative importance of different physical effects.

6. Numerical library

We have developed a numerical library containing various modules that, when coupled, enable multiphysics simulations (see Figures 1, 6 and Refs. [5–9,18–21]). This library, unlike existing

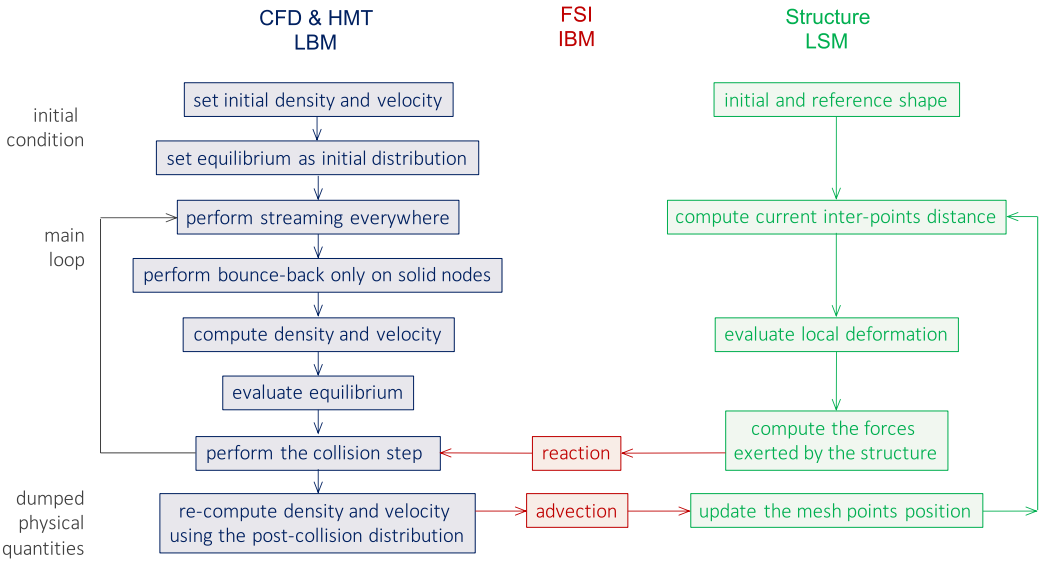

Figure 6. Flowchart summarizing the algorithm describing the sequence of the execution steps for each block of the code: LBM, LSM and IBM, as well as the coupling levels between them.

commercial and open-source software, is better suited for biomedical applications involving transport phenomena at the mesoscopic scale. It allows for coupling between the dynamics of complex fluids and deformable structures, as well as mass or heat transfer and the consideration of external stimuli.

For the simulation of fluid flow and mass or heat transfer, we have developed the *lbm2d* (2D simulations: https://gitlab.utc.fr/kaouibad/lbm2d) and *lbm3d* (3D simulations: https://gitlab.utc.fr/kaouibad/lbm3d) modules based on the LBM method. For the fluid–structure interaction, we have developed the *ibm2d* (https://gitlab.utc.fr/kaouibad/ibm2d) and *ibm3d* (https://gitlab.utc.fr/kaouibad/ibm3d) modules based on the IBM method. For computing the structure deformation, we have developed modules based mainly on the LSM method. For the post-processing, we have developed the *io3d* module (https://gitlab.utc.fr/kaouibad/io3d), which allows reading and writing output files in VTK format (https://vtk.org). These files are readable by the open-source software ParaView (https://www.paraview.org) that allows 3D visualization of the results (e.g., structure, streamlines, or concentration fields). The functions in the library are programmed in modern Fortran language. The 2D codes are parallelized using CAF (Co-Array Fortran), which is better suited for work stations with shared memory, while the 3D codes use MPI (Message Passing Interface), a more appropriate parallelization method for supercomputers with distributed memory.

Figure 7 shows the performance of the *lbm3d* module on the Jean Zay supercomputer of the IDRIS institute of the CNRS. The case study involves simple shear flow between two walls (https://gitlab.utc.fr/kaouibad/examples), computed in a 3D domain of size $400 \times 42 \times 42$ (a total of 705,600 points), with a total of 2000 time iterations. The performance of the *lbm3d* solver on the Jean Zay supercomputer demonstrates strong scalability across a range of CPU counts. The measured speed-up closely follows the ideal linear trend, indicating efficient parallelization and effective utilization of computational resources. While the solver maintains near-linear speed-up at lower to moderate CPU counts, a slight deviation from ideal performance is observed as the number of CPUs increases, which is typical due to factors such as communication overhead.

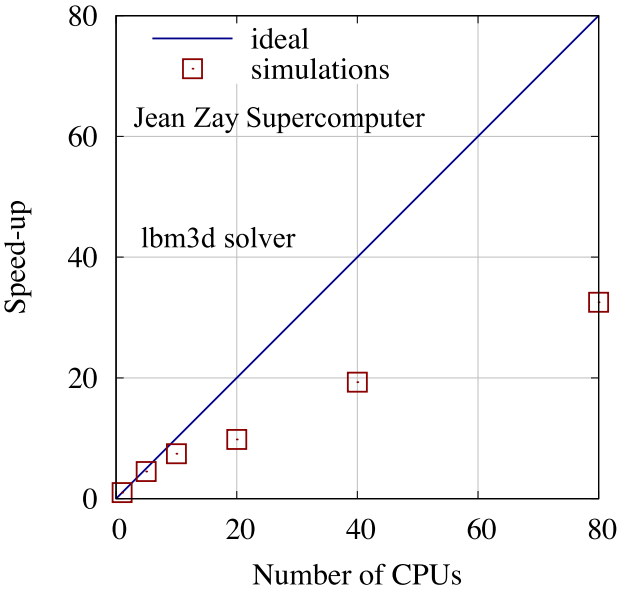

Figure 7. Performance of the *lbm3d* solver on Jean Zay supercomputer of IDRIS institute of CNRS. The straight line indicates linear speed-up: perfect scaling.

Overall, the *lbm3d* solver exhibits high parallel efficiency, making it well-suited for large-scale simulations on modern high-performance computing architectures.

7. Applications

We limit ourselves to show only three applications from our ongoing research projects:

(i) 3D simulation of drug release from a capsule subjected to external shear flow (cf. Figure 8). This simulation allows for predicting the spatial distribution of the released molecules, which is altered by the capsule dynamics and the resulting flow. This pharmaceutical application involves coupling between the flow of the internal and the external fluids of the capsule, the advection–diffusion of the solute, and the fluid–structure–solute coupling [9,21]. The fluid transports the solute by advection, while the solute itself has no direct influence on the flow.

(ii) 3D simulation of the performance of an organ (pancreas) on a microfluidic chip (Organ-On-Chip), cf. Figure 9. A spheroid composed of pancreatic cell aggregates, modeled by a suspended sphere, is trapped and maintained in one of the wells of a microfluidic chip. This spheroid secretes insulin, which is transported by the ambient flow within the device. This bioengineering problem requires computing fluid flow in a complex geometry: a microfluidic system with wells designed to trap the spheroids [22]. It relies also on simulating fluid interaction with the sphere, and two advection–diffusion–reaction equations: one for insulin dynamics and the other for glucose. These last two equations are coupled by source terms based on a feedback mechanism: the glucose level carried by the ambient fluid stimulates and controls the degree of insulin secretion by the spheroid.

(iii) 3D simulation of the dynamics of a valve composed of two crescent-shaped leaflets (cf. Figure 10). The valves described here are typical of the vessels in the lymphatic system. This biological system relies on strong coupling between several phenomena: the deformation of structures (vessels and lymphatic valves), fluid–structure interactions, and the transport of

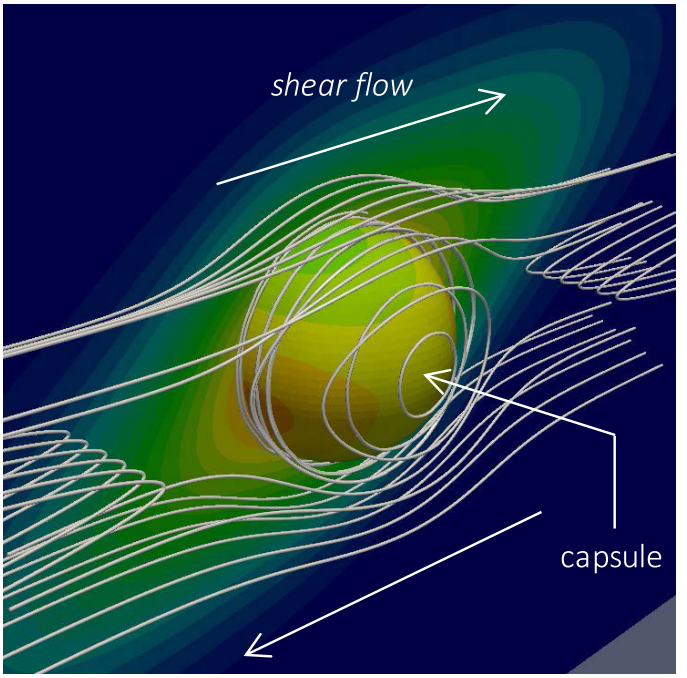

Figure 8. Drug release from a capsule subjected to shear flow. The simulation allows for analyzing the spatial distribution of the released molecules and the flow developed around the capsule.

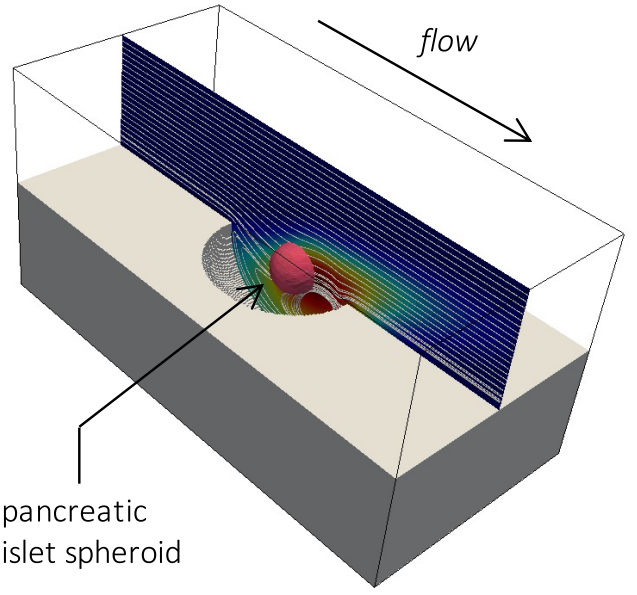

Figure 9. Suspended spheroid trapped by one of the wells of a microfluidic chip operating as an artificial pancreas. The simulation predicts the dynamics of the spheroid under flow within the well, as well as the spatial distribution of the secreted insulin.

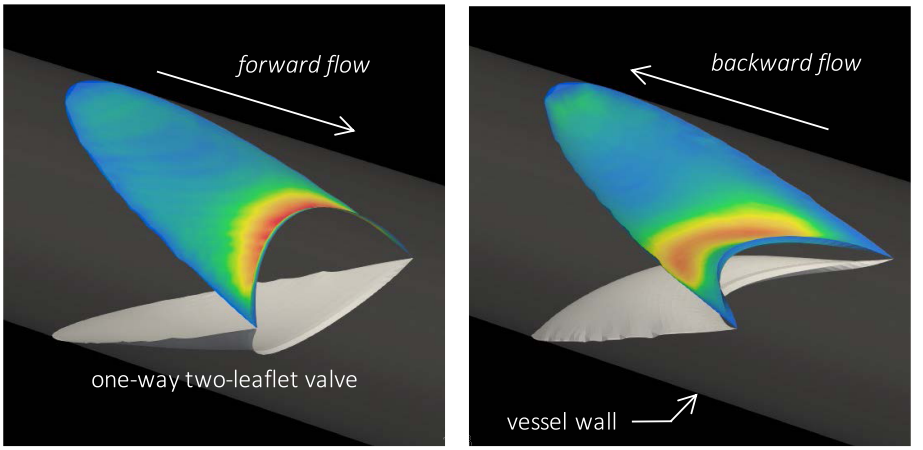

Figure 10. Opening (on the left) and closing (on the right) of a bicuspid lymphatic valve under the effect of oscillatory flow. The simulation also allows for analyzing the spatial distribution of wall shear stress on the surface of one of the valve's leaflets.

biochemical entities such as calcium ions (Ca^{2+}) and nitric oxide (NO). Unlike other fluid mechanics applications, the flow in this context is not imposed. It is instead generated by a complex mechanism involving the synchronization between the opening and closing of the lymphatic valves and the contraction and relaxation of the walls of the lymphatic vessels, which are themselves regulated by biochemical signals. This mechanism ensures the drainage of lymph, the fluid circulating in the lymphatic system [23]. The simulation in Figure 10 shows the opening and closing of a lymphatic valve, as well as the prediction of the distribution of wall shear stresses on the surface of one of the leaflets.

The source codes used to produce the results for the three applications can be provided upon request by contacting the author via email.

8. Conclusions

We have presented the development and application of modern numerical methods to study complex fluid–structure interaction problems coupled with transport phenomena, with a particular focus on biomedical applications. The combination of LBM, LSM and IBM methods allows for an efficient approach to model multiphysics problems at the mesoscopic-scale. The applications, such as drug release from particles, organ-on-chip and lymphatic valves, demonstrate the versatility and potential of these tools in addressing the challenges posed by modern biomedical applications. Moreover, the developed numerical library offers a flexible, modular and high-performance alternative to commercial software. These works open promising perspectives for the study of complex biological, biomedical and biomimetic systems, and could also find applications in other scientific and industrial fields such as materials science, chemical engineering, and environmental engineering. In the future, the integration of other numerical methods, along with the use of machine learning approaches, could further complement and expand the range of applications.

Declaration of interest

The author does not work for, advise, own shares in, or receive funds from any organization that could benefit from this article, and has declared no affiliations other than his research institution.

Acknowledgments

The author thanks his students, colleagues, collaborators, as well as the National Research Agency for funding the MechLymph (ANR-20-CE45-0008-01), UC-DC (ANR-23-CE51-0057) and SOCA (ANR-24-CE06-6245-02) projects. High-performance simulations were carried out on the PILCAM2 supercomputers (https://pilcam2.utc.fr) at UTC and Jean-Zay at CNRS, thanks to the allocation of computing time provided by GENCI-IDRIS (Grant 2024-[AD012A13687R2]).

References

[1] S. Succi, *The Lattice Boltzmann Equation for Fluid Dynamics and Beyond*, Oxford University Press: Oxford, 2001.
[2] M. C. Sukop and D. T. Thorne, *Lattice Boltzmann Modeling*, Springer: Berlin, 2006.
[3] C. K. Aidun and J. R. Clausen, "Lattice–Boltzmann method for complex flows", *Annu. Rev. Fluid Mech.* **42** (2010), pp. 439–472.
[4] Q. Zou and X. He, "On pressure and velocity boundary conditions for the lattice Boltzmann BGK model", *Phys. Fluids* **9** (1997), pp. 1591–1598.
[5] B. Kaoui, "Flow and mass transfer around a core-shell reservoir", *Phys. Rev. E* **95** (2017), article no. 063310.
[6] B. Kaoui, "Computer simulations of drug release from a liposome into the bloodstream", *Eur. Phys. J. E* **41** (2018), no. 2, article no. 20.
[7] B. Kaoui, "Algorithm to implement unsteady jump boundary conditions within the lattice Boltzmann method", *Eur. Phys. J. E* **43** (2020), article no. 23.
[8] B. Kaoui and J. Harting, "Two-dimensional lattice-Boltzmann simulations of vesicles with viscosity contrast", *Rheol. Acta* **55** (2016), no. 6, pp. 465–475.
[9] C. Bielinski, L. Xia, G. Helbecque and B. Kaoui, "Mass transfer from a sheared spherical rigid capsule", *Phys. Fluids* **34** (2022), article no. 031902.
[10] M. Ostoja-Starzewski, "Lattice models in micromechanics", *Appl. Mech. Rev.* **55** (2002), no. 1, pp. 35–60.
[11] T. Omori, T. Ishikawa, D. Barthès-Biesel, A.-V. Salsac, J. Walter, Y. Imai and T. Yamaguchi, "Comparison between spring network models and continuum constitutive laws: application to the large deformation of a capsule in shear flow", *Phys. Rev. E* **83** (2011), no. 4, article no. 041918.
[12] R. Kusters, T. van der Heijden, B. Kaoui, J. Harting and C. Storm, "Forced transport of deformable containers through narrow constrictions", *Phys. Rev. E* **90** (2014), article no. 033006.
[13] T. Krüger, B. Kaoui and J. Harting, "Interplay of inertia and deformability on rheological properties of a suspension of capsules", *J. Fluid Mech.* **751** (2014), pp. 725–745.
[14] C. Bielinski, O. Aouane, J. Harting and B. Kaoui, "Squeezing multiple soft particles into a constriction: transition to clogging", *Phys. Rev. E* **104** (2021), article no. 065101.
[15] C. S. Peskin, "The immersed boundary method", *Acta Numer.* **11** (2002), pp. 479–517.
[16] R. Verzicco, "Immersed boundary methods: historical perspective and future outlook", *Annu. Rev. Fluid Mech.* **55** (2023), pp. 129–155.
[17] R. Mittal and J. H. Seo, "Origin and evolution of immersed boundary methods in computational fluid dynamics", *Phys. Rev. Fluids* **8** (2023), article no. 100501.
[18] B. Kaoui, *Modelling vesicle dynamics in extended geometries and in microfluidic devices*, PhD thesis, University of Joseph Fourier: Grenoble, France, 2009.
[19] B. Kaoui, J. Harting and C. Misbah, "Two-dimensional vesicle dynamics under shear flow: effect of confinement", *Phys. Rev. E* **83** (2011), article no. 066319.
[20] B. Kaoui, *Interaction fluide-structure couplée aux phenomènes de transport dans des systèmes biologiques et biomédicaux*, Habilitation à Diriger des Recherches (HDR), Université de Technologie de Compiègne: Compiègne, France, 2022.
[21] C. Bielinski and B. Kaoui, "Transfert de masse non-stationnaire depuis des particules sous écoulement", *C. R. Méca.* **351** (2023), pp. 1–12.
[22] A. Essaouiba et al., "Microwell-based pancreas-on-chip model enhances genes expression and functionality of rat islets of Langerhans", *Mol. Cell. Endocrinol.* **514** (2020), article no. 110892.
[23] T. P. Padera, E. F. Meijer and L. L. Munn, "The lymphatic system in disease processes and cancer progression", *Annu. Rev. Biomed. Eng.* **18** (2016), pp. 125–158.